Appl Biochem Biotechnol (2015) 175:825–840
DOI 10.1007/s12010-014-1299-y

Cytotoxic and Genotoxic Effects of Titanium Dioxide Nanoparticles in Testicular Cells of Male Wistar Rat

Ramovatar Meena · Kumari Kajal · Paulraj R.

Received: 6 February 2014 / Accepted: 15 October 2014 /
Published online: 25 October 2014

Abstract Serious concerns have been expressed about potential risks of engineered nanoparticles. Regulatory health risk assessment of such particles has become mandatory for the safe use in consumer products and medicines; also, the potential effects on reproduction and fertility are relevant for this risk evaluation. In the present study, we examined the effects of intravenously injected titanium dioxide nanoparticles (TiO_2-NPs; 21 nm), with special emphasis on reproductive system. Antioxidant enzymes such as catalase, glutathione peroxidase, and superoxide dismutase showed a significant decrease, while significant increase in lipid peroxidase was observed. Our results confirmed the bioaccumulation of TiO_2-NPs in testicular cells. In TiO_2-NPs-treated animals, various functional and pathological disorders, such as reduced sperm count, increase in caspase-3 (a biomarker of apoptosis), creatine kinase activity, DNA damage, and cell apoptosis were observed. Moreover, the testosterone activity was decreased significantly in a dose-dependent manner in the animals treated with TiO_2-NPs as compared with control group animals. It is concluded that TiO_2-NPs induce oxidative stress, which produce cytotoxic and genotoxic changes in sperms which may affect the fertilizing potential of spermatozoa.

Keywords TiO_2 nanoparticles · Oxidative stress · Sperm cytotoxicity

Introduction

Nanoparticles have a particle size of one dimension that is less than 100 nm. These are produced daily by anthropogenic activities such as drinking, cooking, and generating energy in power plants. Engineered nanoparticles are used in sporting goods, tires, stain- resistant clothing, sunscreens, clothing's, electronics, and in medicine for the purpose of diagnosis and drug delivery [1–4]. Nanotoxicology, an evaluation of the safety of engineered nanostructures and nanodevices, is a novel field of toxicology. Materials that are generally thought to be inert may act differently when introduced to the body as nanomaterials [5–7]. Among the varieties of engineered nanoparticles being used today, titanium dioxide (TiO_2) nanoparticles

R. Meena · P. R. (✉)
School of Environmental Sciences, Jawaharlal Nehru University, New Delhi, India 110067
e-mail: paulrajr@hotmail.com

K. Kajal
International Centre for Genetic Engineering and Biotechnology, New Delhi, India 110067

are one of the most widely used in consumer products. They are extensively used in cosmetics and sunscreens because of their efficient UV absorption properties without scattering the visible light. This makes them transparent and more aesthetically acceptable as compared with their bulk counterpart [8]. Our previous study reported that intravenously injected nano-TiO_2 induce oxidative stress which produces genotoxicity such as oxidative DNA damage, micronuclei induction, and cell apoptosis in liver and kidney [9]. Gurr et al. [10] reported that nanosized anatase TiO_2 particles induced oxidative DNA damage, lipid peroxidation, and micronuclei formation and increased cell apoptosis in HEK-293 cells (human embryonic kidney cell line), even in absence of photoactivation.

Reproductive organs are very sensitive to stress such as heavy metals, xenobiotics compounds, microwaves, and nanoparticles. It is well documented that NPs are able to cross the blood–testes and blood–brain barriers [11, 12]. Mouse Leydig cells possess a large capacity for the internalization of nanoparticles, and these nanoparticles induce cytotoxicity and gene expression changes that lead to impairment of male mouse reproductive system [13, 14].

Earlier studies pertained to cytotoxicity on male germ line cells [15, 16] assessed deposition and bioaccumulation of nanoparticles in testes, as well as reproductive outcomes in successive offspring over one and half years. It was found that, after injection or ingestion of nanoparticles, there is translocation systemically from primary sites of entry to across the blood–testes barrier, and deposition and bioaccumulation in testes [17, 18]. Furthermore, the presence of small amounts of nanoparticles has also been shown in the glands and interstitial cells of mammalian testes [17]. Additionally, there is evidence that germ line sperm cells can be damaged due to exposure to metal nanoparticle [15].

During spermiogenesis, apoptosis plays a key role in adjusting the appropriate number of proliferating germ cells associated with the surrounding Sertoli cells. Regulation of apoptosis is based on the intracellular dominance of various proteins that induce or inhibit the apoptotic process, such as BAX, Bcl, caspase-3, and several key enzymes [19]. Caspases are present as inactive precursors and activated by initiator caspase through autoactive proteolysis [20]. The initiator caspases 8 and 9 with effector caspase 3 are considered the main executors of apoptosis [21]. The effector caspase 3 share both pathways, the mitochondrial pathway through caspase 9 and the death-receptor pathway through initiator caspase 8 [22].

Creatine kinase is a marker of sperm maturity, and its elevated level is associated with an increased rate of functional abnormalities and increased cytoplasmic retention [23]. Creatine kinase catalyses the reversible phosphorylation of their ADP to ATP or creatine to creatine phosphate, thus maintaining an immediately accessible energy reservoir in the cell [24]. Creatine phosphokinase supplies the ATP to sperm, a key enzyme in transport and synthesis of energy [25]. Sperm is frequently associated with elevated activities of certain key enzymes, including creatine kinase, which are indicators of male infertility [26–28].

However, little attention has been focused on the health impact of nanoparticles, in particular, the cytotoxic and genotoxic effects of TiO_2-NPs on reproductive organs. Hence, the present investigation is aimed to explore the possible impact of TiO_2-NPs on reproductive systems.

Materials and Methods

Chemicals

Glutathione reduced, glutathione reductase, β NADPH (nicotine amine adenine dinucleotide phosphate-oxidase), 5,5'-dithiobis (2-nitrobenzoic acid), pyrogallol, propidium iodide, sodium

dihydrogen orthophosphate, TritonX-100, thiobarbituric acid, trichloroacetic acid (TCA), RNase, proteinase K, low-melting-point agarose), dimethyl sulfoxide, and titanium dioxide nanoparticles were purchased from Sigma Aldrich, USA. The rest of the chemicals were procured from local chemical companies.

Characterization of Nanoparticles

TiO_2-NPs (50 μg/ml) were dissolved in distilled water and ultrasonicated for 10 min to make the homogeneous suspension. Average particle size, morphology, and size distribution of TiO_2-NPs were examined by a JEOL-JEM-2100 F transmission electron microscope (TEM) operating at 200 kV. The diameters of randomly selected particles were measured at ×15,000 magnification. The aqueous suspension was drop-casted on a carbon-coated copper grid, and the grid was air-dried at room temperature (25 ° C) before loading into the microscope. The TiO_2-nano was further characterized by X-ray diffraction (XRD). The XRD patterns (Bragg peaks) were recorded with a PANalytical X'pert PRO diffractometer using a solid-state detector with a monochromatized Cu kα1 (λ_{Cu}=1.54A°) radiation source at 45 kV.

Animal Treatment

Eight-week-old male Wistar rats were used to evaluate the reproductive cytotoxicity and genotoxicity of TiO_2-NPs. Animals were divided randomly into four different groups, with six animals in each group (control, 5, 25, and 50 mg/kg). Animals of treated group were injected intravenously (through caudal vein) for 30 days at weekly interval with different doses of TiO_2-NPs dissolved in 1 M phosphate buffered saline (PBS). Control group animals were injected with 1 M PBS. All the experiments were performed as per the guidelines of the Institutional Animal Ethical Committee.

Preparation of Tissue Homogenates

After nanoparticle treatment, animals were sacrificed, and testis was removed and washed with PBS and frozen in liquid nitrogen and store at −80 °C. The tissues were rinsed in chilled Tris–KCl buffer (0.15 M pH 7.4) and made 10 % homogenates (1 gm tissue in 10 ml Tris–KCl buffer) and centrifuged at 14,000 rpm for 30 min at 4 °C. Supernatant was used for enzymatic analysis such as catalase, Superoxide dismutase, glutathione peroxidase, and lipid peroxidase.

Quantification of Titanium

Testis of all animals were removed, weighed, and incinerated at 200 °C for 20 min. Press-powdered samples were prepared by using 10 tons pressure to the sample; boric acid was used with organ powder as a supporter base. Titanium concentration was analyzed in 1 g sample with energy dispersive X-ray fluorescence spectroscopy (Epsilon5 PANalytical) [9].

Antioxidative Enzyme Activity

Superoxide Dismutase Assay

Superoxide dismutase (SOD) activity was determined as per the method of Marklund and Marklund [29]. The supernatant was diluted ten times with sodium phosphate buffer (0.1 M, pH 7.4) and treated with 1 % Triton-x-100 and kept at 4 °C for 30 min, followed by addition of

1 ml of assay mixture containing 0.05 M sodium phosphate buffer (pH 8), 0.01 M EDTA, and 0.27 mM pyrogallol. The absorbance was observed for 2 min at 420 nm using UV–visible spectrophotometer (CARY, 100 Bio). The enzyme activity was expressed as units per milligram protein, where 1 U is the amount of enzyme required to bring about 50 % inhibition of the auto-oxidation of pyrogallol.

Catalase Assay

Catalase (CAT) activity was measured in the samples according to the method of Aebi [30]. The supernatant was diluted ten times with sodium phosphate buffer (0.1 M, pH 7.4) and 1 % Triton-X 100 was added along with 10 μl of ethanol. Then, the mixture was incubated on ice for 30 min. The reaction mixture (1 ml) consisted of 3 μM H_2O_2 in phosphate buffered saline and 0.02 ml of incubated sample. The optical density was measured at 240 nm for a period of 120 s in the spectrophotometer. Catalase activity was expressed as nano-Kat per milligram protein. (One Kat is defined as 1 mole of H_2O_2 consumed per second per milligram protein).

Glutathione Peroxidase Assay

Glutathione peroxidase (GSH-Px) activity in supernatant was measured according to the method of Mills [31]. The assay mixture consisted 550 μl sodium phosphate buffer (0.1 M, pH7.4), 100 μl NADPH (2 mM), 10 μl glutathione reductase (2 μl in 500 μl buffer), and 10 μl glutathione reduced (9.22 mg/ml). Enzymatic reaction was started by the addition of 25 μl sample (supernatant) and 100 μl hydrogen peroxide, and the absorbance was scanned for 3 min at 340 nm using UV–visible Spectrophotometer. The GPx activity was expressed as micromoles of NADPH oxidized per minute per milligram protein.

Lipid Peroxidation Assay

Lipid peroxidase in microsomes prepared from testis was estimated spectrophotometrically by thiobarbituric acid-reactive substances method as described by Varshney and Kale [32]. In brief, 0.4 ml of microsomal sample was mixed with 1.6 ml of Tris–KCl (0.15 M KCl +10 mM Tris–HCl, pH 7.4) buffer to which 0.5 ml of 30 % trichloroacetic acid was added. Then 0.5 ml of thiobarbituric acid was added. The mixture was incubated at 80 °C for 45 min, cooled on ice, and centrifuged at room temperature for 10 min at 3,000 rpm in Remi-T8 table-top centrifuge. The absorbance of the clear supernatant was measured at 531.8 nm in spectrophotometer. It is expressed in terms of malonaldehyde (MDA) formed per milligram protein.

Creatine Kinase Assay

Creatine kinase levels were measured using the procedure described by Kumar et al. [33]. An aliquot of semen was transferred to a 15-ml conical centrifuge tube. The seminal plasma was removed by washing with ice-cold imidazole buffer [0.15 M NaCl and 0.03 M imidazole (pH 7.0) at a ratio of 1:15(*v*/*v*)]. The supernatant was decanted after centrifugation at 500×*g*, and the pellet was re-suspended in a 0.1 % Triton X-100 detergent solution by vortexing for 20 s. The sample was centrifuged again at 500×*g*, and the creatine kinase (CK) activity of the supernatant was analyzed at 340 nm by spectrophotometer. In this assay, the creatine is enzymatically converted into sarcosine, which is then specifically oxidized to generate a product that converts a colorless probe to an intensely red product. This final product is detected colorimetrically at 340 nm). The CK activity is expressed as units per 10^8 sperm.

Measurement of Caspase-3 Activity

The activity of caspase-3 was measured using the colorimetric assay kit (Sigma Aldrich, USA). The spermatozoa were centrifuged at 2,000 rpm for 10 min at 4 °C. The pellet was then re-suspended in lysis buffer for 20 min and centrifuged at 20,000×*g* for 20 min at 4 °C, and the supernatant was collected. The assay was conducted in 96-well plates. The colorimetric caspase-3 assay is based on the hydrolysis of the peptide substrate acetyl-Asp-Glu-Val-Asp p-nitroanilide (Ac-DEVD-pNA), which results in the release of the p-nitroaniline (pNA) moiety. To assess the specific contribution of caspase-3 activity, the Ac-DEVD–pNA substrate (2 mM) was added to each well according to the instructions of the manufacturer. The plates were incubated overnight at 37 °C to measure the caspase-3 activity. The absorbance was measured using a microplate reader (Spectromax M2) at 405 nm.

Testosterone Assay

A serum testosterone assay was performed using the testosterone enzyme immunoassay (EIA) kit (Cayman, USA). The procedures for the assay were followed as described in the manual of the manufacturer. In brief, 50 ml of the testosterone standard or serum, 50 ml of the testosterone AChE tracer, and 50 ml of the testosterone antiserum were added to the wells of an ELISA plate containing 100 ml of EIA buffer. The sensitivity of the assay was 6 pg/ml. The optical density was noted using spectrophotometer (SpectroMax M2) that was sensitive at a wavelength range of 405–420 nm.

DNA Damage

The DNA damage in sperm cells was measured by comet and DNA fragmentation assay. Sperm cells were harvested from testis and fixed with 1:3 glacial acetic acid/methanol and washed with PBS (1.37 mM NaCl, 4.3 mM Na_2HPO_4, 2.7 mM KCl, 1.4 mM KH_2PO_4, pH 7.4). Single-cell gel electrophoresis was performed as the method of Paulraj and Behari [34]. Cellular DNA damage was visualized under fluorescence microscope (Carl Zeiss) after staining with a fluorescent DNA-binding dye ethidium bromide (EtBr). Fifty cells were randomly selected from each slide of different groups, and the results were analyzed by Comet IV software.

For DNA fragmentation assay, sperm samples (200 μl, 1×10^6cells/ml) were suspended in lysis buffer (50 mM Tris, pH 7.5, 10 mM EDTA, and 0.3 % Triton X-100) for 30 min on ice. DNA ladder assay was conducted according to the method of Gong et al. [35], with slight modification. DNA samples were analyzed by horizontal electrophoresis for 5 h in 2 % agarose gel pre-stained with 1 mmol/L EtBr. The DNA fragmentation was observed under UV light.

Detection of Apoptosis and Total Sperm Count

Fluorescence activated cell sorting (FACS) analysis was carried out to confirm the occurrence of apoptosis (fluorescein isothiocyanate annexin-V+propidium iodide) and total sperm count in the epididymis after TiO2-NPs exposure followed by propidium iodide (PI) staining. Sperm samples (100 μl, 2×10^6cells/ml) were taken in falcon 12×75 mm polypropylene tube with snap cap, and 1 ml ice-cold 70 % ethanol was added. Sample was incubated overnight at 4 °C. After the incubation period, sample was centrifuged at 1,500 rpm for 10 min at 4 °C, and finally, the supernatant was decanted. The 100 μl RNAase (100 units) was added to the pellet

and pipetted thereafter. Samples were incubated at room temperature for 20 min. Finally, these samples were stained with 50 μl (25 μg/ml) PI just prior to the analysis.

Microscopic Analysis of Testis

Brain samples were dissected from animals and fixed in 10 % formalin. Samples were embedded in paraffin, sectioned, and stained with hematoxylin and eosin. Slides were examined by light microscopy and were analyzed blindly by a pathologist. For ultrastructure analysis of brain, small pieces of tissue (~2 mm) were fixed in 2.5 % gluteraldehyde for 4 h and washed in 0.2 M PBS. Post-fixation was done with 1 % osmium tetra-oxide for 1 h. Cells were washed in PBS and dehydrated in alcohol (50 %, 70 %, 80 %, 95 %, and 100 %). Cells were further treated with propylene oxide (30 min), propylene oxide–resin mixture (overnight), and pure resin (48 h). Embedding was done in BEEM (better equipment for electron microscopy) capsules using pure Spurr's low-viscosity resin at 80 °C for 48 h. Ultrathin sections (70 nm) were taken using Leica EMUC-6 ultramicrotom and stained with 1 % lead acetate. Sections were examined under JEOL-JEM-2100 F TEM operating at 200 kV.

Statistical Analysis

SPPX (Statistix version 4.00) was used for computing statistics of the study parameters such as one-way analysis of variance. Difference among the means was considered significant at $p<0.01$ and $p<0.05$ levels.

Results

Characterization of Nano-TiO_2

Transmission electron microscopic images showed that the TiO_2-NPs in clustered suspension had an average diameter of 10–20 nm (Fig. 1a). TiO_2-NPs contained elemental titanium 66 %

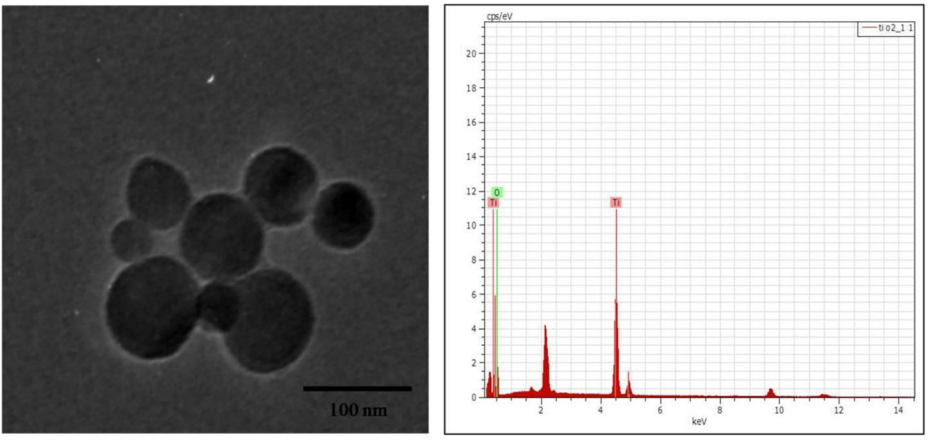

Fig. 1 TEM image of TiO_2-NPs at ×15,000 magnification. **a** The particle size calculated with TEM ranges from 10–20 nm; scale bar size is 100 nm. **b** Energy dispersive X-ray profile (titanium dioxide nanoparticles on copper grid)

and oxygen 34 % atoms (Fig. 1b). The wide-angle region of the XRD patterns of TiO_2-NPs exhibited a high-intensity diffraction peak at 2θ=25.2° and four additional peaks at 2θ=37.7°, 48.0°, 54.7°, and 62.5° (Fig. 2) that were ascribed to 101, 004, 200, 211, and 002 diffractions of tetragonal TiO_2, respectively. The size of TiO_2-NPs calculated on the basis of half angle and the height of peak with XRD was nearly equivalent to the size calculated by TEM (10±2–25± 2 nm).

Coefficient of Organs

There was no significant difference in coefficients of the testis between the lower doses of TiO_2-NP-treated animals and control ones whereas, in animals treated with 50 mg/kg TiO_2-NPs, the average coefficients of testis (13.19±1.54) was significantly ($p<0.05$) decreased as compared with control ones (16.44±1.25), suggesting that a higher dose of TiO_2-NPs might cause the damage of the testis (Fig. 3).

Titanium Content Analysis

TiO_2-NPs may cross the testes–blood barrier and accumulated in testis. This phenomenon showed that the accumulation of titanium in the organs was closely related to organ-to-body-weight ratio. The concentration of titanium in the testis of animals treated with 5, 25, and 50 mg/kg of TiO_2-NPs was 2.16±0.52, 4.6±0.44, and 6.3±0.53 ppm, respectively, whereas in the control group, titanium concentration was 0.74±0.08 ppm (Fig. 4).

Oxidative Stress Parameter

It is proved that the TiO_2-NPs imbalances the homeostasis between reactive oxygen species (ROS)and antioxidants in testicular cells. The activity of antioxidative enzymes like SOD and GPx was decreased in a dose-dependent manner (Fig. 5a). The SOD activity was significantly ($p<0.05$) decreased in 25 and 50 mg/kg of TiO_2-NP-treated

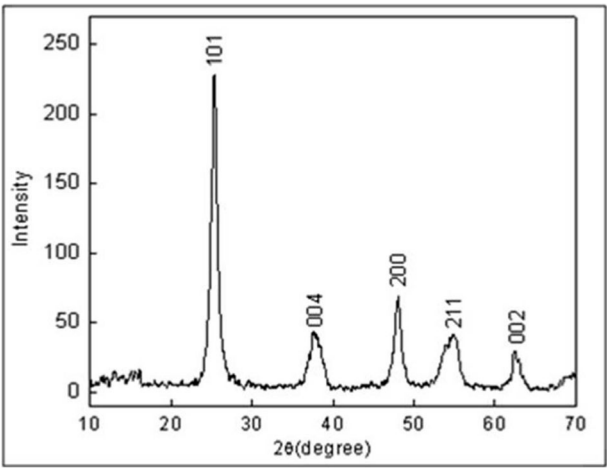

Fig. 2 Powder X-ray diffraction patterns of TiO_2-NPs with Miller indices (h k l) showing crystal family of planes for each diffraction peak

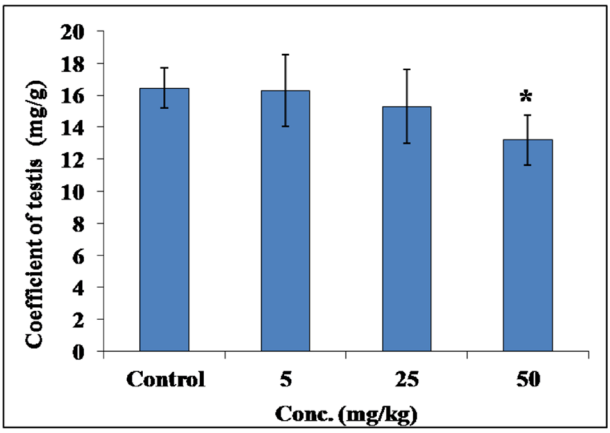

Fig. 3 Coefficient of testis of rat treated with TiO_2-NPs. Data represented as mean±SD. *Indicates statistical significance at $p<0.05$

groups (76.67±9.6 and 55±8.7 U/mg protein, respectively) as compared with control animals (126.67±9.8 U/mg protein). However, a significant increase in CAT activity was observed ($p<0.05$) in 25 and 50 mg/kg of TiO_2-NP-treated groups with respect to the control animals, which indicates that TiO_2-NPs affect the activity of catalase in sperm cells (Fig. 5b). The results illustrated that GPx activity was significantly ($p<0.01$) decreased in a 25 and 50 mg/kg of TiO_2-NP-treated groups (4.23±0.37 and 3.7±0.4 nM of NADPH oxidized/min/mg protein) with respect to the control animals (5.9±0.36 nM/min/mg protein) (Fig. 5c) whereas the lipid peroxidase activity was significantly ($p<0.001$) increased in 25 and 50 mg/kg treated groups (3.39±0.10 and 4.21±0.14 nM MDA/mg protein) as compared with control group (1.97±0.22 nM MDA/mg protein) (Fig. 5d). The reduction of enzymatic activity may be due to TiO_2-NP-induced inhibition of mRNA expression of SOD and GPx, additional evidence

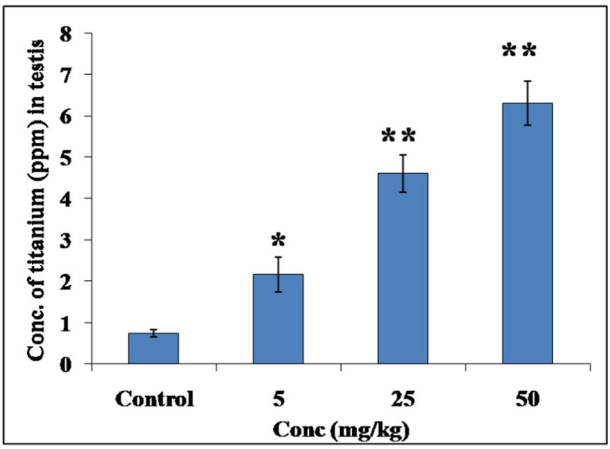

Fig. 4 Concentration of titanium in testis of Wistar rat treated with varying doses of TiO_2-NPs. Data represented as mean±SD. *Indicates statistical significance at ($p<0.05$), **very significant ($p<0.01$)

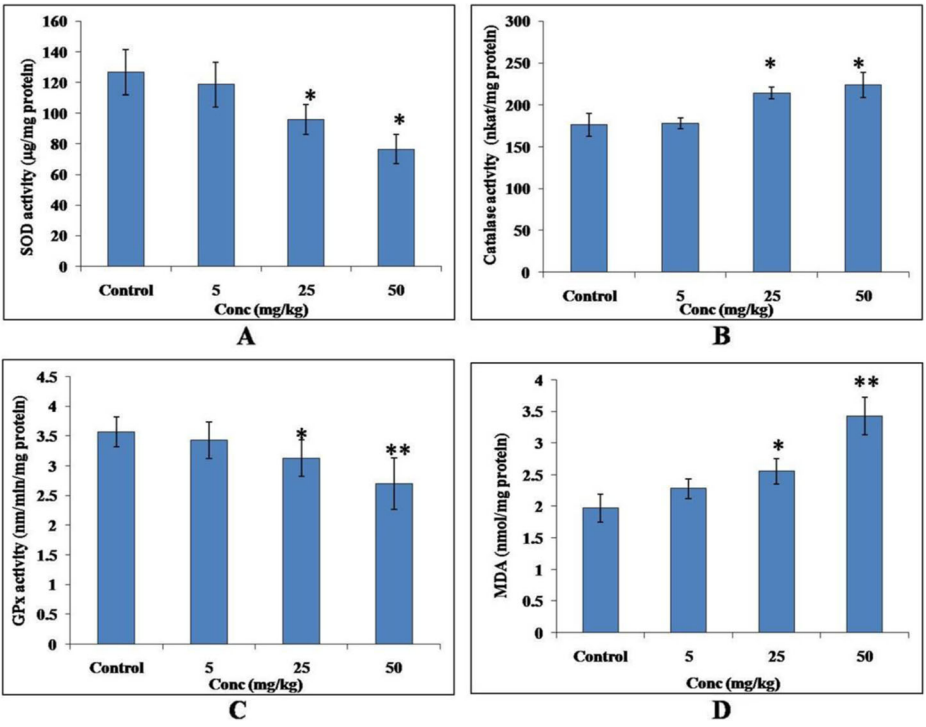

Fig. 5 Shows the comparison of antioxidative enzyme level in testis among the control and TiO_2-NP-treated groups. **a** SOD activity (unit per milligram protein), **b** catalase activity (nano-Kat per milligram protein), **c** GPx activity (nanomoles of NADPH oxidized per minute per milligram protein), **d** LPx activity (nanomoles MDA per milligram protein). Data represented as mean±SD. *Indicates statistical significance at $p<0.05$, **very significant at ($p<0.01$)

pointing to the possibility that oxidative stress was provided by the increase in ROS production and lipid peroxidase levels.

Creatine Kinase Activity

The critical role for CK in sperm energy transport was examined by measuring the ATP concentrations or ATP/ADP ratios. The mean value of the CK level was significantly increased ($p<0.01$) in the sperm from the 50 mg/kg of TiO_2-NP-treated group (0.12±0.01) than in the sperm from the control group (0.04±0.01). There were no significant ($p>0.01$) elevation observed in the 5 and 25 mg/kg of TiO_2-NP-treated groups as compared with the control group (Fig. 6).

Caspase 3 Activity

A statistically significant activation of caspase-3 was observed in higher dose of TiO_2-NP-treated (50 mg/kg) animals (Fig. 7). The sperm caspase-3 activity increased by 1.5-fold in 50 mg/kg of TiO_2-NP-treated group as compared with control group, whereas there were no significant differences of sperm caspase-3 activity between the 5 and 25 mg/kg of TiO_2 NP-treated groups and control group. These results suggest that the TiO_2-NPs at higher concentration induce apoptosis in germ cells.

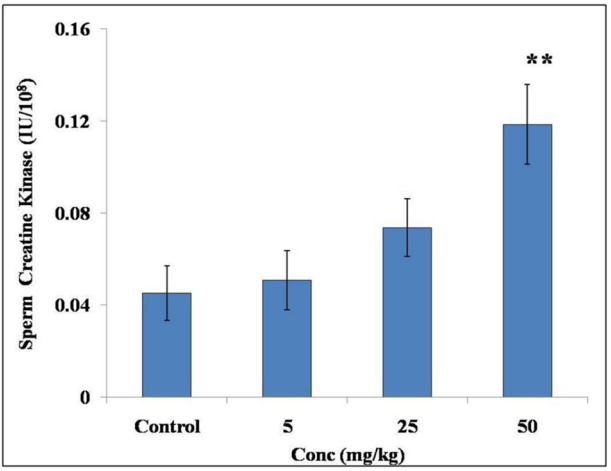

Fig. 6 Represents the creatine kinase (CK) activity distribution in the sperm fractions of various groups treated with different doses of TiO_2-NPs. Results expressed as IU/10^8 spermatozoa±standard deviation. **Indicates statistical significance compared with control counterpart ($p<0.01$)

Serum Testosterone Level

The serum testosterone level decreased significantly ($p<0.01$) in the 50 mg/kg of TiO_2-NP-treated group (4.92±0.37 ng/mg protein) compared with the control group (7.44±0.62). There were no significant differences of sperm testosterone level between the low dose of TiO_2-NP-treated (5 and 25 mg/kg) groups and control groups, which indicates that only a higher dose may affect the sperm testosterone level (Fig. 8).

Assessment of DNA Damage

The comet length (tail length, tail movement, and tail migration) were significantly increased ($p<0.001$) in the higher dose (25 and 50 mg/kg) of TiO_2-NP-treated sperm cells (Fig. 9). These

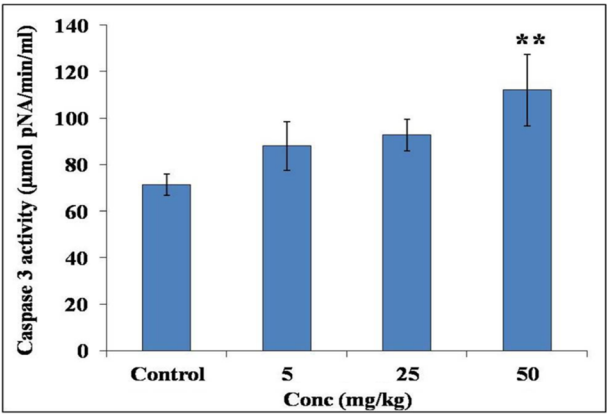

Fig. 7 Shows the comparison of caspase-3 activity in sperm among the control and TiO_2-NP-treated groups. Caspase-3 activity is expressed in micromoles pNA released per minute per milliliter of sperm lysate. Data illustrated as mean±SD. *Indicates statistical significance at $p<0.05$, **very significant at $p<0.01$

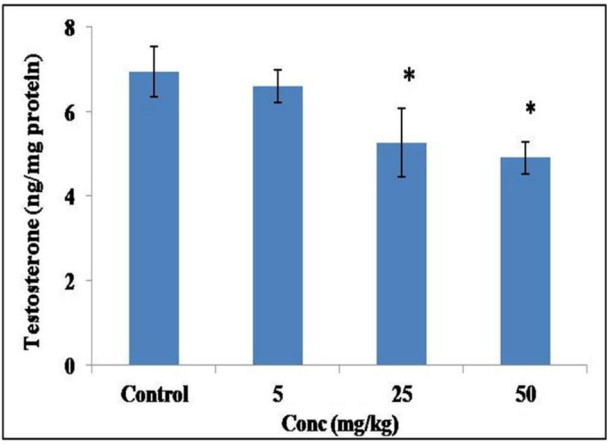

Fig. 8 Comparison of testosterone level among the control and TiO_2-nano-treated groups. Testosterone activity is expressed as nanograms per milligram protein. Results are shown as mean±SD. **Indicates statistical significance compared with control group ($p<0.01$)

results indicated that only higher doses of TiO_2-NPs (25 and 50 mg/kg) induce the DNA damage in sperm cells, while low doses (5 mg/kg) did not cause any DNA damage.

Detection of Total Sperm Count and Cell Apoptosis

The induction of apoptosis was confirmed by DNA fragmentation assay. DNA extracts from sperm cells treated with 50 mg/kg TiO_2-NPs displayed ladder patterns of discontinuous DNA fragments (Fig. 10), but no DNA fragments were detected in control group or in TiO_2-NP-

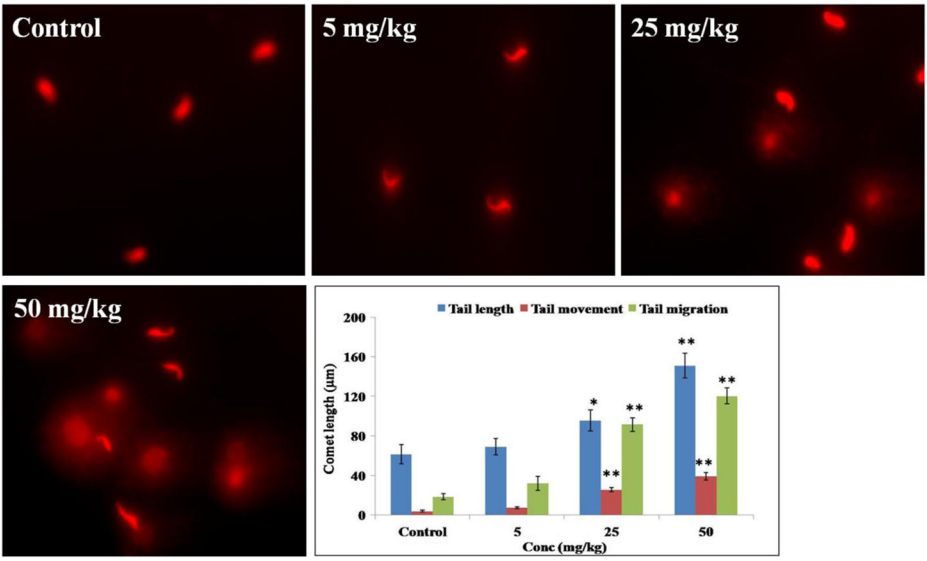

Fig. 9 DNA strand breaks in sperm cells among control and TiO_2-NP-treated Wistar rat. Graph shows comet length of sperm cells among the TiO_2-NP-treated groups and control group. Data shown as mean±SD. *Indicates statistical significance at $p<0.05$, **very significant at ($p<0.01$)

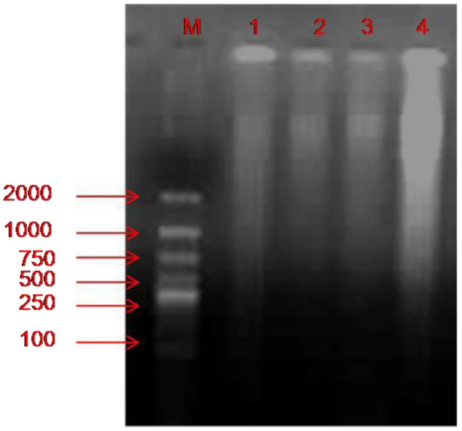

Fig. 10 Showing DNA fragmentation induced by TiO_2-NPs in sperm cells. *Lane M*, low-molecular-weight DNA ladder, *lane 1*, control group; *lane 2*, 5 mg/kg exposed group; *lane 3*, 25 mg/kg exposed group; *lane 4*, 50 mg/kg exposed group

treated groups given lower doses. A significant decrease in total sperm counts was observed in 50 mg/kg TiO_2-NP-treated group as compared with the control group (Fig. 11a). Meanwhile, Fig. 11b shows a significant increase in apoptotic cell population observed in 50 mg/kg TiO_2-NP-treated group as compared with the control group. There was a significant positive correlation between ROS levels and apoptosis in testicular cells (R^2=0.948).

Pathological and Morphological Alterations in Testis

There were no pathological changes observed in 5 and 25 mg/kg treated groups, whereas moderate alterations were found in 50 mg/kg treated groups. The stained section of seminiferous tubules from control rat indicates normal spermatogenic cycle with germ cells and Sertoli cells, whereas nano-TiO_2-exposed rats show abnormal testicular morphology. In exposed rat, some seminiferous tubules appear disorganized and disrupted. Results also indicated some inflammation in testicular cells (Fig. 12).

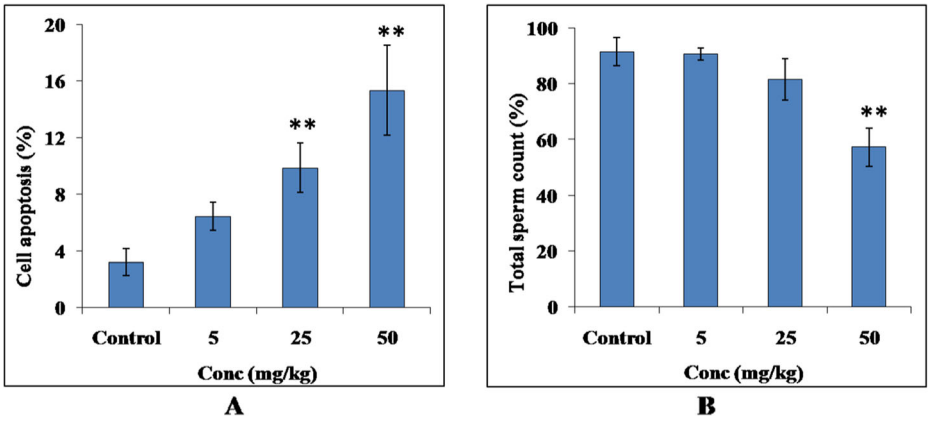

Fig. 11 Effects of various doses of TiO_2-NPs on sperm cells, **a** showing an increased cell apoptosis percentage of male germ cells. Data represented as mean±SD. **Indicates statistically significance with control group (p<0.01), **b** percentage of total sperm count among TiO_2-NP-treated groups and control group. **Indicates statistical significance with control group (p<0.01)

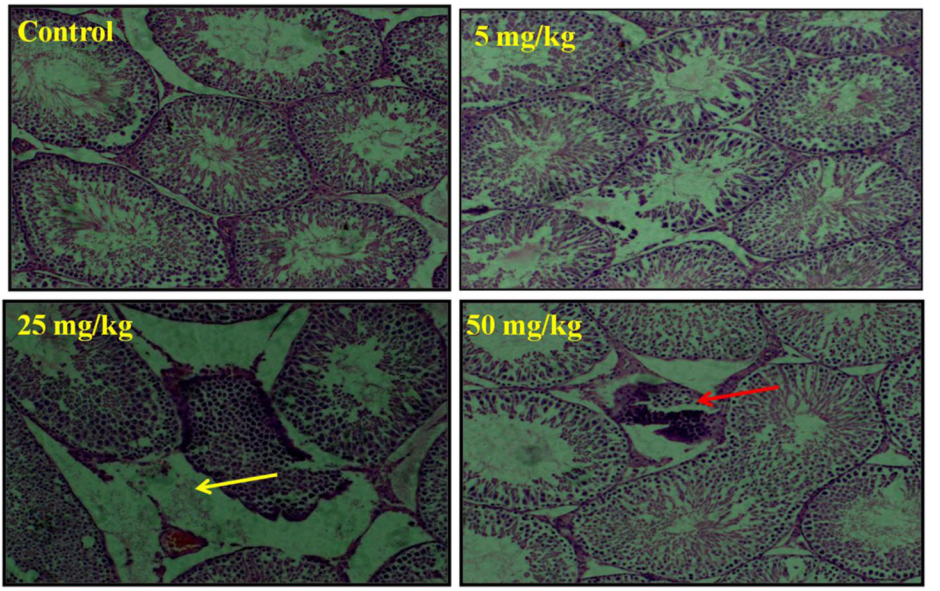

Fig. 12 Hematoxylin-and-eosin-stained sections of somniferous tubules. **a** Control group, **b** 5, **c** 25, and **d** 50 mg/kg of TiO_2-NP-treated groups. *Red arrow* indicates cellular inflammation in testicular cells, and *yellow arrow* indicates the proteomic fluid

Ultrastructural results of testicular cells of treated animals indicate that TiO_2 nanoparticles were localized in the cytoplasm, mostly in membranous compartments, including lysosome and mitochondria, thecal organelles, besides particles existing out of cells, surrounding cells. Compared with control cells, no visible morphological changes were detected in cells exposed to TiO_2-NPs (Fig. 13).

Discussion

Generally, the oxidative stress caused by the particle is considered to be one of the important mechanisms of nanoparticle toxicity, especially for those particles containing transition metals [36]. Based on increasing experimental results [37], it is hypothesized that the respiratory and cardiovascular diseases caused by transition metal or its oxide particle exposure may be due to the induction of ROS. It has been shown that nanoparticles that enter the testis can induce oxidative stress locally. A repeated exposure of TiO_2-NPs for 90 consecutive days induced oxidative stress in testis, a depletion of reduced GSH and oxidized glutathione levels in the testis, as well as inhibition of SOD activity and a slight increase in catalase activity [38].

The results show that the intracellular antioxidant defenses, i.e., CAT, GSH-Px, and SOD, were decreased, whereas lipid peroxidation level significantly increased in testis administered with higher doses of TiO_2-NPs. According to these results, it is clear that TiO_2-NPs induce oxidative stress in the testis, which leads to various cellular damages. ROS is a well known marker of cellular oxidative stress. One month after TiO_2-NPs, MDA levels increased about 1.5- and two-fold in the testis of rat treated with 25 and 50 mg/kg of TiO_2-NPs, respectively.

Previous studies reported that there is a correlation between ROS, lipid peroxidation, and DNA damage in response to toxicants [16, 39]. ROS generation in the testes was responsible

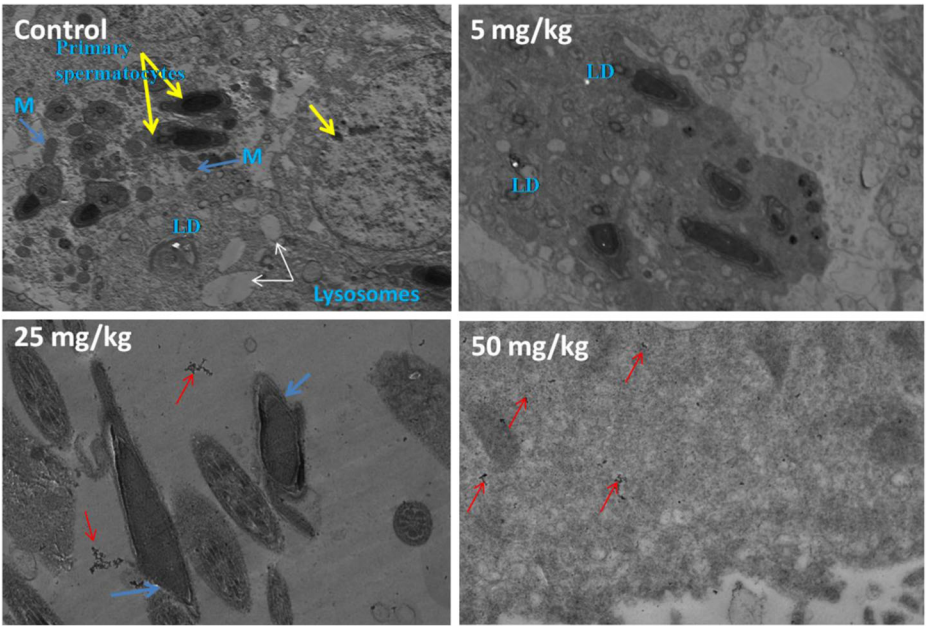

Fig. 13 **a** Shows TEM images of testis of male Wistar rat treated with different doses of TiO_2-NPs. **a** Control group, **b** 5, **c** 25, and **d** 50 mg/kg of TiO_2-NP-treated groups. *Red arrow* indicates clusters of nanoparticles, whereas *blue arrow* shows abnormal mature spermatids. *LD*=lipid droplets, *M*=mitrochondria, *N*=nucleus

for the possible toxic effects on the physiology of reproduction. However, cells have a defense mechanism [i.e., antioxidants (reduced glutathione, catalase, superoxide dismutase)] to fight against increased ROS production. Decreased serum testosterone levels and increased creatine kinase activity were associated with reduced male fertility. Our data reflect an appreciable increase in sperm creatine kinase activity and a decline in the activities of antioxidants. Da-Silva-Paula et al. [40] studied the in vitro effect of silver nanoparticles (AgNPs) on the activity of CK from rat brain, heart, and skeletal muscle and demonstrated that AgNPs (10, 25, and 50 mg/l) inhibited CK from brain and skeletal muscle, but not from heart. They concluded that a decrease of CK activity may impair energy homeostasis, contributing to cell death. Our results indicated that higher dose of TiO_2-NPs significantly changes the activity of CK, which may lead to reduction in mature sperms or functional abnormities. Testosterone was produced in Leydig cells and in supported Sertoli cells. Low levels of testosterone might suppress spermatogenesis because they could lead to dysfunction of the Sertoli cells. Our results were in line with the previous study which showed that exposure to carbon black (CB) nanoparticles induced the dysfunction of Leydig cells, and consequently the fluctuation of serum testosterone levels in the CB nanoparticle-exposed group [13].

Genotoxic stresses induced by nanoparticles trigger an arrest or delay in the G2 phase of the cell cycle to permit the repair of damaged DNA [41]. Cell cycle analysis by flow cytometry with propidium iodide has confirmed that TiO2-NPs induce apoptosis, as shown by sub-G1 apoptotic peak and DNA fragmentation in spermatozoa. Activated caspases commit the cells with defective repair machinery to an apoptotic death by cleaving a number of substrates. The results of the caspase assay suggest that the apoptotic cell counts are significantly increased.

Therefore, apoptosis is considered to be involved in the impairment of spermatogenesis and the seminiferous tubules. Guo et al. [42] demonstrated a significant reduction in sperm density

and motility and an increase in sperm abnormality and germ cell apoptosis in mice treated with intra-peritoneal injections of TiO_2-NPs, whereas no pathological changes were observed in testes and epididymis. Meanwhile, in present study, when rats were intravenously exposed to anatase TiO_2-NPs, NPs were aggregates in Leydig cells, Sertoli cells, and spermatids in the testes. Disorganized and disrupted seminiferous tubules, tubule lumens with few mature sperm, as well as decrease in daily sperm production, epididymal sperm motility, and numbers of Sertoli cells were also observed.

Conclusion

The present study suggests that intravenous administration of higher doses of TiO_2-NPs causes apoptosis during spermiogenesis or sperm maturation, and sperm caspase-3 activity seems to affect the physiology of reproduction. Study has been hypothesized that TiO_2-NPs induce oxidative stress, which causes DNA damage and cell apoptosis. It may be concluded that higher doses of TiO_2-NPs cause various cellular and genetic changes in rat.

References

1. Mazzola, L. (2003). Commercialising nanotechnology. *Nature Biotechnology, 21*, 1137–1143.
2. Paull, R., Wolfe, J., Hebert, P., & Sinkula, M. (2003). Investing in nanotechnology. *Nature Biotechnology, 21*, 1144–1147.
3. Salata, O. V. (2004). Applications of nanoparticles in biology and medicine. *Journal Nanobiotechnology, 2*, 3.
4. Nel, A., Xia, T., Madler, L., & Li, N. (2006). Toxic potential of nanomaterials at the nanolevel. *Science, 311*, 622–627.
5. Donaldson, K., Stone, V., Tran, C. L., Kreyling, W., & Borm, P. J. A. (2004). Nanotoxicology. *Occupational and Environmental Medicine, 61*, 727–728.
6. Hoet, P. H. M., Bruske-Hohlfeld, I., & Salata, O. V. (2004). Nanoparticles known and unknown health risks. *Journal Nanobiotechnology, 2*, 12.
7. Oberdorster, G., Oberdorster, E., & Oberdorster, J. (2005). Nanotoxicology: an emerging discipline evolving from studies of ultrafine particles. *Environmental Health Perspectives, 113*, 823–839.
8. Newman, M. D., Stotland, M., & Ellis, J. I. (2009). The safety of nanosized particles in titanium dioxide–and zinc oxide–based sunscreens. *Journal of the American Academy of Dermatology, 61*(4), 685–692.
9. Meena, R., & Paulraj, R. (2012). Oxidative stress mediated cytotoxicity of TiO_2 nano anatase in liver and kidney of Wistar rat. *Toxicological and Environmental Chemistry, 94*(1), 146–163.
10. Gurr, J., Wang, A. A. S., Chen, C., & Jan, K. (2005). Ultrafine titanium dioxide particles in the absence of photoactivation can induce oxidative damage to human bronchial epithelial cells. *Toxicology, 213*, 66–73.
11. De Jong, W. H., Hagens, W. I., Krystek, P., Burger, M. C., Sips, A. J., & Geertsma, R. E. (2008). Particle size-dependent organ distribution of gold nanoparticles after intravenous administration. *Biomaterials, 29*, 1912–1919.
12. Lankveld, D. P., Oomen, A. G., Krystek, P., Neigh, A., Troost-de, J. A., Noorlander, C. W., Van Eijkeren, J. C., Geertsma, R. E., & De Jong, W. H. (2010). The kinetics of the tissue distribution of silver nanoparticles of different sizes. *Biomaterials, 31*, 8350–8361.
13. Yoshida, S., Ono, N., Tsukue, N., Oshio, S., Umeda, T., Takano, H., & Takeda, K. (2006). In utero exposure to diesel exhaust increased accessory reproductive gland weight and serum testosterone concentration in male mice. *Environmental Sciences, 13*, 139–147.
14. Asare, N., Instanesa, C., Sandberga, W. J., Refsnesa, M., Schwarzea, P., Kruszewskib, M., & Brunborg, G. (2012). Cytotoxic and genotoxic effects of silver nanoparticles in testicular cells. *Toxicology, 291*, 65–72.
15. Braydich-Stolle, L., Hussain, S., Schlager, J. J., & Hofmann, M. C. (2005). In vitro cytotoxicity of nanoparticles in mammalian germline stem cells. *Toxicological Sciences, 88*(2), 412–419.
16. Ema, M., Kobayashi, N., Naya, M., Hanai, S., & Nakanishi, J. (2010). Reproductive and developmental toxicity studies of manufactured nanomaterials. *Reproductive Toxicology, 30*, 343–352.
17. Chen, Y., Xue, Z., Zheng, D., Xia, K., Zhao, Y., Liu, T., Long, Z., & Zia, J. (2003). Sodium chloride modified silica nanoparticles as a non viral vector with a high efficiency of DNA transfer into cells. *Current Gene Therapy, 3*, 273–279.

18. Kim, J. S., Sung, J. H., Ji, J. H., Song, K. S., Lee, J. H., Kang, C. S., & Yu, I. J. (2011). In vivo genotoxicity of silver nanoparticles after 90-day silver nanoparticle inhalation exposure. *Safety Health Work, 2*, 34–38.
19. Cayli, S., Sakkas, D., Vigue, L., Demir, R., & Huszar, G. (2004). Cellular maturity and apoptosis in human sperm: creatine kinase, caspase-3 and Bcl-XL levels in mature and diminished maturity sperm. *Molecular Human Reproduction, 10*, 365–372.
20. Ceruti, S., Beltrami, E., Matarrese, P., Mazzola, A., Cattabeni, F., & Malorni, W. (2003). A key role for caspase-2 and caspase-3 in the apoptosis induced by 2-chloro-2'-deoxy-adenosine (cladribine) and 2-chloro-adenosine in human astrocytoma cells. *Molecular Pharmacology, 63*, 1437–1447.
21. Riedl, S. J., & Shi, Y. (2004). Molecular mechanisms of caspase regulation during apoptosis. *Nature Reviews Molecular Cell Biology, 5*, 897–907.
22. Pommier, Y., Sordet, O., Antony, S., Hayward, R. L., & Kohn, K. W. (2004). Apoptosis defects and chemotherapy resistance: molecular interaction maps and networks. *Oncogene, 23*, 2934–2949.
23. Hallak, J., Sharma, R. K., Pasqualotto, F. F., Ranganathan, P., Thomas, A. J., & Agarwal, A. (2001). Creatine kinase as an indicator of sperm quality and maturity in men with oligospermia. *Urology, 58*, 446–451.
24. Wallimann, T., Moser, H., Zurbriggen, B., Wegmann, G., & Eppenberger, H. M. (1986). Creatine kinase isoenzymes in spermatozoa. *Journal of Muscle Research and Cell Motility, 7*, 25–34.
25. Kavanagh, J. P., & Darby, C. (1983). Creatine kinase and ATPase in human seminal fluid and prostatic fluid. *Journal of Reproduction and Fertility, 68*, 51–56.
26. Huszar, G., Corrales, M., & Vigue, L. (1988). Correlation between sperm creatine phosphokinase activity and sperm concentrations in normospermic and oligospermic men. *Gamete Research, 19*, 67–75.
27. Huszar, G., Vigue, L., & Corrales, M. (1988). Sperm creatine phosphokinase activity as a measure of sperm quality in normospermic, variablespermic, and oligospermic men. *Biology of Reproduction, 38*, 1061–1066.
28. Huszar, G., & Vigue, L. (1993). Incomplete development of human spermatozoa is associated with increased creatine phosphokinase concentration and abnormal head morphology. *Molecular Reproduction and Development, 34*, 292–298.
29. Marklund, S., & Marklund, G. (1974). Involvement of the superoxide anion radical in autoxidation of pyrogallol as a convenient assay for superoxide dismutase. *European Journal of Biochemistry, 47*, 469–474.
30. Aebi, H. (1974). Catalase. In Bergmeyer (ed.), *Methods of Enzymatic. Analysis, 2*, 673–684. New York: Academic Press.
31. Mills, G. C. (1959). The purification and properties of glutathione peroxidase of erythrocytes. *Journal of Biological Chemistry, 234*, 502.
32. Varshney, R., & Kale, R. K. (1990). Effect of calmodulin antagonist on radiation-induced lipid peroxidation in microsomes. *International Journal of Radiation Biology, 58*, 733–743.
33. Kumar, S., Kesari, K. K., & Behari, J. (2011). The therapeutic effect of a pulsed electromagnetic field on the reproductive patterns of male Wistar rats exposed to a 2.45-GHz microwave field. *Clinics, 66*(7), 1237–1245.
34. Paulraj, R., & Behari, J. (2006). Single strand DNA breaks in rat brain cells exposed to microwave radiation. *Mutation Research, 596*, 76–80.
35. Gong, J. P., Traganos, F., & Darzynkiewicz, Z. (1994). A selective procedure for DNA extraction from apoptotic cells applicable for gel electrophoresis and flow cytometry. *Analytical Biochemistry, 218*(2), 314–319.
36. Tiwari, D. K., Jin, T., & Behari, J. (2011). Dose-dependent in-vivo toxicity assessment of silver nanoparticle in Wistar rats. *Toxicology Mechanisms and Methods, 21*(1), 13–24.
37. Simeonova, P. P., & Lusster, M. T. (1995). Iron and reactive oxygen species in the asbestos-induced tumour necrosis factor a response from alveolar macrophages. *American Journal of Respiratory Cell and Molecular Biology, 12*(6), 676–683.
38. Zhao, X., Sheng, L., Wang, L., Hong, J., Yu, X., Sang, X., & Hong, F. (2014). Mechanisms of nanosized titanium dioxide-induced testicular oxidative stress and apoptosis in male mice. *Particle and Fibre Toxicology, 11*(1), 47.
39. Chaudhari, M., Jayaraj, R., Bhaskar, A. S. B., & Lakshmana, R. (2009). Oxidative stress induction by T-2 toxin causes DNA damage and triggers apoptosis via caspase pathway in human cervical cancer cells. *Toxicology, 262*, 153–161.
40. Da Silva Paula, M. M., da Costa, C. S., Baldin, M. C., Scaini, G., Rezin, G. T., Segala, K., & Streckb, E. L. (2009). In vitro effect of silver nanoparticles on creatine kinase activity. *Journal of the Brazilian Chemical Society, 20*(8), 1556–1560.
41. Hemmati, P. G., Normand, G., Gillissen, B., Wendt, J., Dorken, B., & Daniel, P. T. (2008). Cooperative effect of p21Cip1/WAF-1 and 14-3-3sigma on cell cycle arrest and apoptosis induction by p14ARF. *Oncogene, 27*, 6707–6719.
42. Guo, L. L., Liu, X. H., Qin, D. X., Gao, L., Zhang, H. M., Liu, J. Y., & Cui, Y. G. (2009). Effects of nanosized titanium dioxide on the reproductive system of male mice. *National Journal of Andrology, 15*(6), 517.